Dual Driven Mechanism (Hygro-Redox) Semi-IPN Composite Film (Polyaniline-Polyacrylic Acid/ Sulfonated Poly (Ether Ether Ketone) for Artificial Muscles

Haval Kareem [1*], Alex Langrock [1], Jeffrey Auletta [1], Luther Mahoney [1, 4], Daniel Hallinan [2], Hyun Kim [1, 5], Asher C. Leff [1, 3], Dat T. Tran [1], and David Mackie [1]

[1] Sensors and Electron Devices Directorate, DEVCOM Army Research Laboratory, Adelphi, MD 20783, USA
[2] Department of Chemical and Biomedical Engineering Florida A&M University–Florida State University (FAMU-FSU) College of Engineering, Tallahassee, FL 32310, USA
[3] General Technical Services, Wall Township, NJ 07727, USA
[4] Fibertek Inc., Herndon, VA 20171, USA
[5] Advanced Materials Division, Korea Research Institute of Chemical Technology, Daejeon 34114, Republic of Korea

(* - To whom correspondence should be addressed: haval.r.kareem.civ@army.mil)

Abstract

Different weight ratios of polyaniline (PANI) to poly (acrylic acid) (PAA) were synthesized as interpenetrating polymer networks and blended with sulfonated poly (ether ether ketone) (SPEEK). In-situ polymerization was performed by chemical oxidation of aniline in the presence of PAA. The composites showed actuation capability in the presence of fuel/air and moisture. Mechanical testing indicated that samples with higher concentration of PAA were stronger. For instance, $PANI_1PAA_2SPEEK_3$ breaks at 8.4 MPa and has a failure strain of 2.5 %, which is higher than $PANI_3PAA_1SPEEK_3$ at 7 MPa and 2%. However, higher amount of PAA resulted in a lower electrochemical conductivity of 1.52 x 10^{-2} S/cm for the former and 1.8 x 10^{-2} S/cm for the latter. Intermolecular interaction at the optimum composition is necessary to induce forward and reverse bending of catalyst coated composite under exposure of fuel and air. In addition, the formation of compact structures and rough surfaces resulted in the maximal contractile strain of 1% for $PANI_3PAA_1SPEEK_3$ based on moisture actuation.

Keywords: Semi-IPN Composite, Polyaniline (PANI), Polyacrylic Acid (PAA), Sulfonated Poly (Ether Ether Ketone) (SPEEK, moisture actuation, redox actuation, Artificial Muscles.

1 Introduction

The exploration of interpenetrating polymer networks (IPNs) to introduce materials with high conductivity, enhanced stability, flexibility, and good mechanical properties have attracted enormous attention.[1-3] IPNs are a promising means to optimize physical and chemical properties and to tackle shortcomings of PANI based composites that have been used in many applications including energy storage, solar cells, electrochemical devices, and artificial muscles.[4-6] PANI has many outstanding properties including reversible doping-dedoping chemistry, and it is well-known for its intrinsic conductivity which varies based on dopants.[7,8] The conductivity of PANI is ascribed to it being a π-conjugated system where the alternating single and double bonds of the PANI chain allow free movement of electrons.[9,10] However, brittleness, weak mechanical properties, poor electrochemical stability, and solubility issues of PANI in organic solvent limit its use in applications.

On the other hand, while soft polymers such as PAA possess poor electrochemical properties, many of their other properties are advantageous. PAA shows good elasticity behavior and it has the capability to absorb more than 100 times its own weight in water due to the presence of COOH groups. As such, a combination of a rigid, field due to the ionic repulsion between the anionic charged groups.[11] Combinations of rigid and conductive polymer such as PANI with PAA in an intimate mingling is a unique way to ensure a synergistic network [8] that enables large volume expansion and contraction under different stimuli, e.g., pH, moisture, temperature, and electric soft polymers have attracted considerable attention because of their potential use in robotics applications as they resemble the physiology of animals dermis where the rigid collagen fibers interact with soft elastin fibers to form a resilient and stretchy material. For example, a rigid

polypyrrole (PPy) was combined with a soft polyol-borate to form a network that has water sensitivity to induce rapid expansion and contraction, where the polyol-borate was responsible for water sorption and desorption inside the PPy resulting in quick and continuous locomotion.[12]

PANI is doped by PAA through acid-base interactions. The modification results in a strong chemical reaction forming a strong adhesion force between the polymer chains. Embedment of the doped PANI in a host matrix such as polymethacrylate, polyvinyl alcohol (PVA), and poly (ether ether ketone) (PEEK) is a secondary interaction leveraged for ease of fabrication. It ensures further enhancement in conductivity and mechanical properties. However, these materials, including PEEK, are insoluble at room temperature in most organic solvents and have poor proton conductivity.[13] There are many methods to enhance solubility and conductivity such as acetalization and application of heat treatment. However, acetalization is not cost effective, and the solubilizing effect of heat treatment is not permanent.[14] Here, in this study, the PEEK is modified through sulfonation with sulfuric acid. Carboxylate groups in PAA increase hydrophilicity while the SPEEK enhances ionic conductivity through sulfonate groups, increases hydrophilicity, boosts the mechanical properties, and helps with film casting.[15]

Catalysis plays a significant role in artificial muscle techniques by converting chemical or electrical energy to mechanical motion. Combinations of nanoparticles and polymers facilitate artificial muscle development. For example, incorporation of gold nanoparticles into electrospun polymer has been shown to help with increasing conductivity.[16,17] In another study, deposition of catalysts on polymers was used with PAN fibers to increase conductivity as a direct electrode, resulting in a 40% change in PAN muscle length in less than 10 minutes under application of electric field.[18] Unlike electronic electroactive polymers which require high voltage, actuation of ionically conductive electroactive polymers can be achieved based on various mild external stimuli

such as heat, light, pH, and electrochemistry.[19,20] For moisture-based actuation, mass uptake and release results in polymer volume change due to the polymer molecular distance change,[21] while for electrochemical driven actuation, the redox process causes electrostatic expulsion between polymer chains as result of ion movement in and out of the polymer network.[22] In the present work, the prepared semi-IPN composite of PANI and PAA with different weight ratio are mixed with SPEEK. A key novelty of this work is preparation of a composite that has capability of conformational change based on electrochemical activation and moisture stimulation. In comparison to a singular stimuli actuator, the system has clear advantages in robotics applications in terms of actuation in response to different stimuli. The results of this work appear to fulfill the prerequisites required of a moisture and chemical based- actuator.

2 Experimental Section

2.1 Materials

Aniline, poly (acrylic acid, Mw = 450000) (PAA), Ammonium persulfate (APS), platinum nanoparticle loaded on carbon 40% (Pt/C), sulfuric acid (H_2SO_4), hydrochloric acid (HCl), and perchloric acid ($HClO_4$) were purchased from Sigma -Aldrich. 2-butanone from, Alfa-Aesar, and FKM (Solvay S. A.). Polyether ether ketone (PEEK) was received from Victrex. All chemicals were used as received

2.2 Sulfonation of Poly (Ether Ether Ketone) (PEEK)

The SPEEK was obtained by dissolving the PEEK in concentrated H_2SO_4 at 60 ºC for 24 hours. Then water was added to induce the phase inversion process. The contents were filtered and washed with water to remove traces of H_2SO_4. Then the collected product was left to dry overnight. The sulfonation degree was determined to be 68% using a classical titration method, in which the test films were soaked in a known concentration and volume of NaOH for 48 hours to

be fully neutralized. The remaining excess of NaOH was back-titrated with known concentration of sulfuric acid.

2.3 Synthesis of PANI-PAA-SPEEK

A modified method of a protocol reported earlier was followed for fabrication of PANI/PAA.[23] The composites were synthesized through chemical oxidative method using perchloric acid as the solvent. Aniline polymerization is exothermic, so to ensure an efficient synthesis and to control heat generation, the polymerization took place in a stirred ice bath (0-5 ºC). The monomer of aniline was added dropwise in the presence of PAA, then ammonium persulfate was slowly added to initiate the in-situ polymerization of aniline. The color of the solution changed gradually from brown to black, indicating complete oxidation of aniline. To produce the maximum molecular weight, the polymerization was carried out over a period of 12 hours.[24] The reactor contents were filtered and washed with a mixture of acetone and water, then the product was dried at 70 ºC. Resulting PANI/PAA IPNs were blended with SPEEK. Controlled weight ratios of PANI/PAA/SPEEK were dissolved in 1 molar perchloric acid. Films were obtained by casting the composite solutions in petri dishes, followed by evaporation of the solvent at 70 ºC.

2.4 Preparation of Films for Actuation Testing

The films were soaked at least for 24 hours in 1M HCl(aq.) to protonate the solid electrolyte structure. The films were, then, dried at room temperature, and were cut into (1 cm X 4 cm) strips. Then, the self-sticking conductive copper foil was attached to the one side of the warm film.

The catalyst ink prepared was made from 40%Pt/C, 2-butanone, and FKM binder. A typical catalyst ink preparation involved dissolving 2.0g (1.05 mL) FKM binder in 98.0g (121.7 mL) of 2-butanone in closed vessel with Teflon-coated stir-bar agitating closed vessel for 1-2 days of

stirring at room temperature. Next, 1.84g of 40%Pt/C was added to the clear FKM solution (2 wt.% FKM in 2-butanone). Then, the closed vessel was sonicated for at least 30 minutes in ice-water.

2.5 Mass Uptake

The assembled films were soaked in 1 molar hydrochloric acid at room temperature for 3 hours. The soaked film were taken out and rinsed with deionized (DI) water and wiped with a tissue to remove residue of acid and weighed immediately. The mass uptake percentage was calculated by the following equation

$$W = (W_s - W_d)/W_d \times 100 \quad (1)$$

where W_s and W_d are the mass of soaked and dry membrane, respectively.

2.6 Characterization

PerkinElmer Lambda 650 S UV-Vis spectrometer was used to obtain UV-Vis spectra. The films were cut into circular shapes and each placed in a quartz sample holder. The measurements were done over the 200-800 nm wavelength range. An FEI Quanta 200F scanning electron microscope (SEM) was used for surface morphology characterization. Powder X-ray diffraction (XRD) patterns were recorded by using a Rigaku Ultima III diffractometer (Cu Kα radiation) in the 2θ range from 1 to 40 degrees with a scan rate of 1 degree per minute. Conductivity/AC impedance measurements were performed via the two probe technique using a computer controlled electrochemical workstation CHI 760E over a frequency range of 0.1 Hz and100 kHz. Mechanical properties were determined using a universal testing machine (ADEMT, eXpert 7601). Films were cut from the cast films of dimensions (20 mm x 5 mm x 0.2 mm) and stretched at a constant rate of 0.1 mm/min until failure (grip separation rate = 2 mm/min). Young's modulus was determined

from the initial slope of the stress-strain curve from 0.5-1.0% strain and the ultimate tensile strength was taken as the maximum stress prior to failure.

3 Results and Discussion

3.1 Composite and Characterization

After the synthesis and casting process, shown schematically in Figure 1, each film was peeled from the petri dish. The top surface of the films showed a rough morphology, whereas the bottom surface was much smoother. Among different compositions, in this work, films with four different weight ratios, $PANI_1PAA_1SPEEK_3$ (A-1), $PANI_2PAA_1SPEEK_3$ (A-2), $PANI_1PAA_2SPEEK_3$ (A-3), and $PANI_3PAA_1SPEEK_3$ (A-4) were synthesized. Note that the three times weight ratio of the host SPEEK to PANI-PAA was necessary to obtain films without fractures and cracks. Also, a higher ratio of PAA resulted in unstable composites, readily soluble in water and ethanol. The functional group or the negative species of the weak polyanion PAA was used as a dopant to overcome the stiffness of PANI owing to its rigid backbone.[25] The intermolecular hydrogen bond and strong electrostatic interaction between anion radicals (COO^-) of PAA and cation radicals (NH_3^+) results in the formation of semi-IPNs with enhanced mechanical properties.[26] The SPEEK makes a significant contribution in enhancement of the conductivity and stretchability through formation of hydrogen bonds and electrostatic interactions. Furthermore, the formation of hydrogen bonds assists with restoration of the original form through dissipation of mechanical energy under stress.[27]

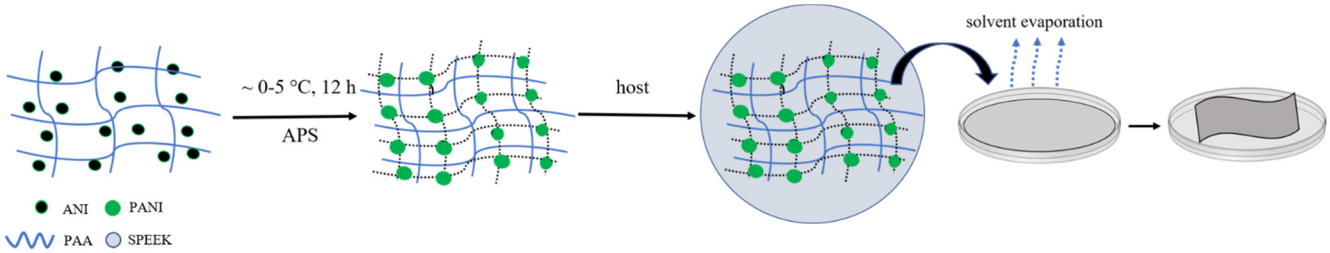

Figure 1 Schematic illustrations of semi-IPN composite preparation protocol

The as-prepared films show excellent mechanical flexibility. Unlike the PANI strip which is brittle and cracks when it is bent, the PANI-PAA-SPEEK films can be twisted and bent freely indicating synergistic network effect (Figure S1)

To investigate the presence of PANI in the composite, UV-Vis spectroscopy was employed. In the UV-vis spectra, the absorption peaks detected at 350-450 nm are attributed to the π-π* transition and polaron-π*, and the band at 550-700 nm is consistent with the polaron-π interaction,[28,29] which is a characteristic of protonation of the emeraldine salt form of PANI (Figure2 A).[30]

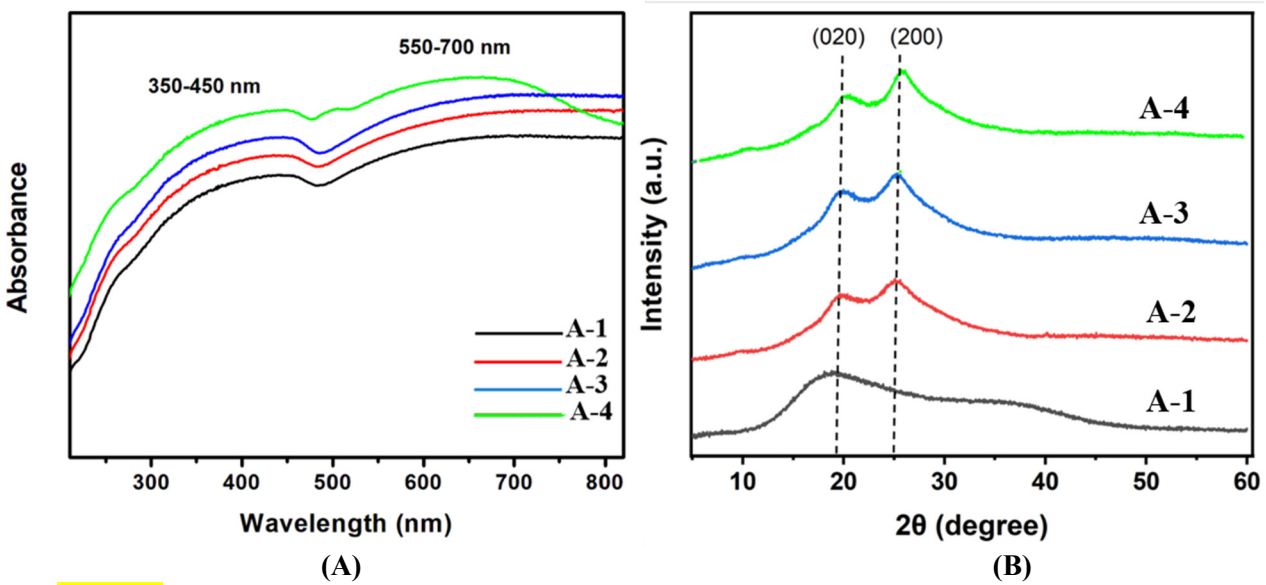

Figure 2 UV-Vis spectra (A), and XRD patterns (B) of as-synthesized for $PANI_1PAA_1SPEEK_3$ (black, A-1), $PANI_2PAA_1SPEEK_3$ (red, A-2), $PANI_1PAA_2SPEEK_3$ (blue, A-3), and $PANI_3PAA_1SPEEK_3$ (green, A-4)

To examine the phases of the composites, powder diffraction (XRD) pattern was employed. Figure 2B shows a set of X-ray diffraction patterns of the PANI-PAA-SPEEK samples with different compositions. The diffraction peaks at ~20º and 25º were assigned to PANI (020), and (200) respectively. [26,31] The assigned peaks of PANI are not shifted for PANI/PAA with different ratios, indicating that the composites are free from impurities and that no other organics generated

due to the interaction between PANI and PAA.[32] The intensity of the diffraction peaks increases as the percentage of PANI increases indicating strong interaction of the components, resulting in a well aligned chain interaction between the composites. As can be seen from Figure2B, the crystallinity is less pronounced in composite A-1. This indicative of more interactions between PANI and PAA with a higher composition. The SEM image in Figure 3, show rough and irregular surfaces for the synthesised PANI-PAA-SPEEK composites with obvious porosity of 10-15 µm in size distributed inconstantly along the samples. Formation of porosity may be linked to trapped air bubbles as a result of solvent evaporation during the film preparation.[27] Vacuum degassing helped with the removal of the air bubbles, however, some remained due to the viscosity of the solution. As can be observed from the SEM images, segregation of the PANI and PAA-SPEEK is less pronounced in A-4 than in the other composites, suggesting that the intermolecular interactions between the components was adequate and resulted in a more compact structure.

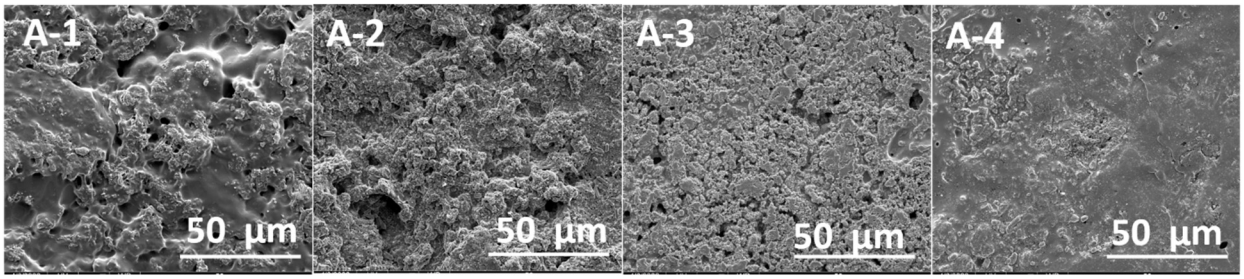

Figure 3: SEM images showing the surface morphology for $PANI_1PAA_1SPEEK_3$ (A-1), $PANI_2PAA_1SPEEK_3$ (A-2), $PANI_1PAA_2SPEEK_3$ (A-3), and $PANI_3PAA_1SPEEK_3$ (A-4)

The two-probe method was used to determine the conductivity of the membranes. The test was performed following the immersion of the samples in 1 molar hydrochloric acid for 4 hours. The conductivity test of the membranes was performed by measuring the resistance R by sandwiching the membranes between two electrodes via AC impedance spectroscopy over a frequency range of 0.1 Hz-100 kHz in room temperature. (Derivation of R from the frequency-

dependent impedance is discussed below.) The following expression was used to measure the conductivity

$$\sigma = L/RA \qquad (2)$$

where L is the thickness of the membrane, and A is the membrane area. The conductivity data of the films shows a clear dependence on the composition, displaying an increase in the order of A-1 < A-3 < A-2 <A-4 as shown in Figure 4A. Having conductivity of 1.8 x 10^{-2} S/cm, A-4 is a considerable improvement in comparison with the reported conductivity value of PANI-PAA (10^{-3} S/cm).[26] The enhanced conductivity property is believed to be linked to the contribution of many factors including intermolecular hydrogen bonds, electrostatic interactions, and that the presence of carboxylate groups contributing to charge transfer along the network. In addition, it was suggested that the optimized molar ratio of PAA resulted in an increase of aniline units along the PANI segment during polymerization.[33]

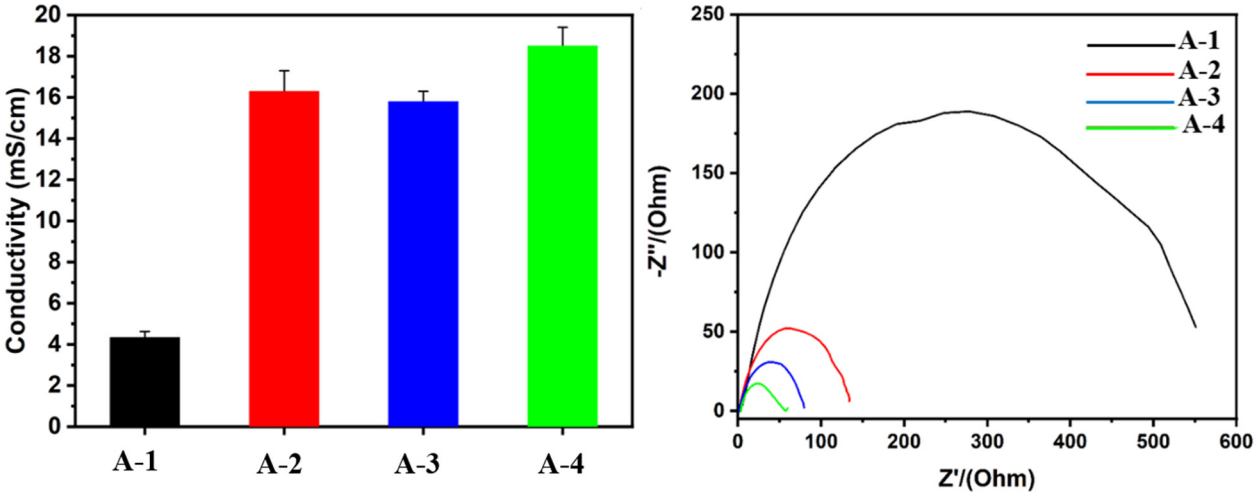

(A) (B)

Figure 4 Conductivity test (A); and impedance test (C) for $PANI_1PAA_1SPEEK_3$ (black, A-1), $PANI_2PAA_1SPEEK_3$ (red, A-2), $PANI_1PAA_2SPEEK_3$ (blue, A-3), and $PANI_3PAA_1SPEEK_3$ (green, A-4)

The interaction between PANI and PAA is governed by the acidity and the microscopic surroundings of the reactants. Due to low acidity of PAA and low basicity of PANI, only a small

portion of carboxylic acid groups of the PAA interact with PANI.[23] Hence, optimizing the composition of PANI/PAA is critical to obtaining a robust composite with enhanced conductivity. Furthermore, addition of SPEEK clearly boosted the conductivity in comparison to bipolymer PANI-PAA in previous reported data.[26] Incorporation of sulfonic groups into the polymer structure via treatment with concentrated sulfuric acid enhances proton conductivity, controls water uptake, and prevents mechanical deterioration.[34] The contribution of SPEEK in conductivity enhancement is dependent on the sulfonation degree. The average degree of sulfonation (DS) achieved was 68%, close to the ideal 70% since lower DS reduces the conductivity and higher DS decreases the polymer resistance [35] and increases water uptake to a degree that negatively affects the reversible contraction of the polymer.[36] The impedance of the composites was determined by sandwiching the films between the electrodes and the frequency was scanned between 0.1 Hz and100 kHz. Figure 4B shows a Nyquist plot where the semi-circle indicates charge-transfer resistance and double-layer capacitance of the electrode.[28] The depressed semicircle indicates roughness and irregularities at the electrode/membrane surface. The imaginary part which prevails at lower frequency is used to characterize the impedance of the composites due to the contribution of the uncompensated resistance to the real part of impedance at higher frequency.[15,37] As can be seen from Figure4C, the data showed the lowest semicircle for sample A-4 followed by A-3, A-2, and A-1. The lower semicircle diameter represents faster electron kinetics within the high frequency region.[38]

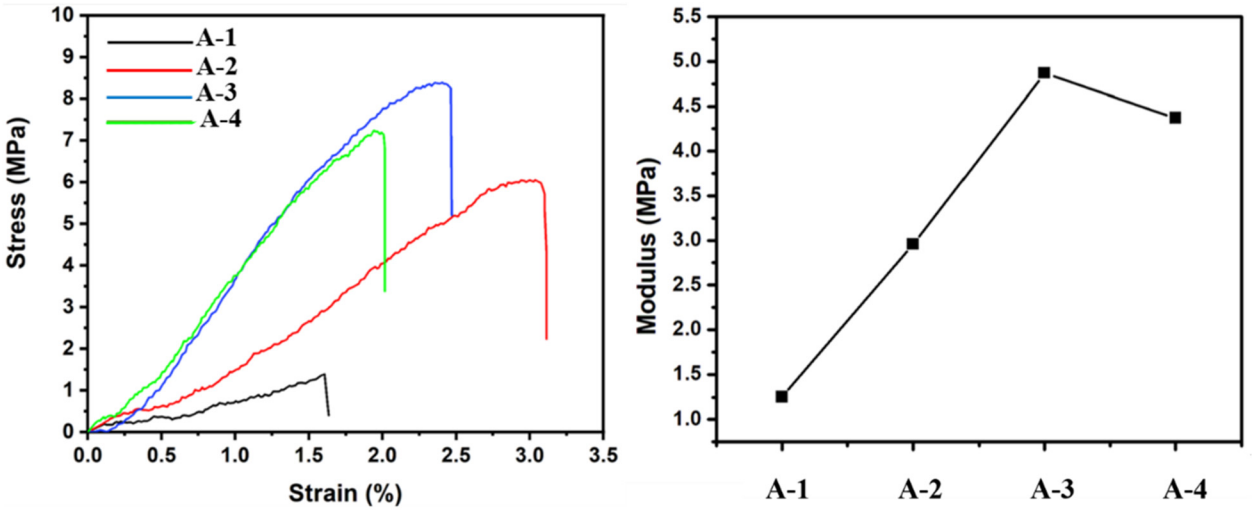

(A) (B)

Figure 5 Stress-strain curves (A), and Young's Modulus (B); for $PANI_1PAA_1SPEEK_3$ (black, A-1), $PANI_2PAA_1SPEEK_3$ (red, A-2), $PANI_1PAA_2SPEEK_3$ (blue, A-3), and $PANI_3PAA_1SPEEK_3$ (green, A-4). The standard deviation is ±

The mechanical properties of the samples at different compositions are shown in Fig 5A and summarized in Table 1. All tensile stress-strain measurements were conducted in the dry state at ambient conditions. The ultimate tensile strength of sample A-3 was the highest measured at 8.4 MPa and failure strain was 2.5%, greater than sample A-4 at 7 MPa and 2%, while sample A-1 was 1 MPa and 1.7%, lower than sample A-2 at 5.5 MPa, which exhibited the highest failure strain at 3.1%. The mechanical property of sample A-3 is attributed to higher PAA content and therefore greater ductility than the samples with a greater fraction of more brittle PANI. The mechanical properties were further assessed by determination of Young's modulus as shown in Figure 5B from the initial slope of the stress-strain curve from 0.5-1.0% strain. The calculated Young's modulus for sample A-3 is 4.75 MPa, higher than that of sample A-4 at 4.37 MPa, sample A-2 at 2.96 MPa, and sample A-1 at 1.25 MPa, indicating the importance of the PAA composition effect in terms of controlling flexibility and strength. Nevertheless, higher concentrations of PAA resulted in an unstable composite with lower electrochemical conductivity. The optimum composition of the composite resulted in a dense structure resistive to defect formation through

development of crosslinked network of hydrogen bonds and intermolecular interaction. Note that physical differences including brittleness and slight powdery touch were observed for film A-1, indicative of inhomogeneity and lack of interaction between the composite's components, which in turn affected the mechanical properties.

Table 1 Mechanical parameters of $PANI_1PAA_1SPEEK_3$ (A-1), $PANI_2PAA_1SPEEK_3$ (A-2), $PANI_1PAA_2SPEEK_3$ (A-3), and $PANI_3PAA_1SPEEK_3$. The standard deviation is ±

Composites	Young's modulus (MPa)	Tensile strength (MPa)	Elongation to failure (%)
A-1	1.25	1.0	1.7
A-2	2.96	5.5	3.1
A-3	4.75	8.4	2.5
A-4	4.37	7.0	2.0

3.2 Redox potential actuation

To test the actuation capability based on redox potential, the samples were cut into rectangular (1 cm x4 cm) strips and attached to an adhesive copper tape backing to form a bilayer bending actuator. Their front sides were then coated with carbon loaded platinum to allow direct conversion of the fuel. The catalyst ink was added dropwise onto copper foil bonded polymeric strips. The copper foil-polymeric strip was clamped on edge to allow free movement of the film while adding to the hexanes soak strip 10 drops of 6 mg Pt/mL of catalyst with a drop approximately 0.02 mL (See Figure S2). The resulting film had approximately 0.3 mg Pt/cm^2 loading. Next, the film was subjected to gentle breeze of air with the chemical fume hood to quickly evaporate the 2-butanone solvent, which to reduce or prevent dissolution of the s-IPN. To firmly attach copper foil to s-IPN, the copper foil-polymeric strip was pressed between aluminum foil-Teflon sheets at 5000 psi for 30 seconds at 100 °C. The aluminum foil-Teflon-copper-polymeric catalyst ink coated film-Teflon-aluminum foil prevents bleed through of the s-IPN into the Teflon sheet. The resulting copper foil-polymeric-catalyst ink structure was trimmed, soaked in deionized water for at least 10 minutes followed by placing in the actuation test reactor system.

After re-sealing the actuation reactor chamber, initial actuation tests were completed with wet (moist) argon or dry argon. The gas flow rate for all gases was calibrated (with glass column) to be 3.1 L/minute (STP). With several wet Ar/dry Ar cycles completed, then, wet H_2 was passed for 30 seconds. Next, wet (or dry) Ar was passed for 30 seconds followed by 30 seconds of dry oxygen Typically, three full cycles were completed for each strip. A full-cycle comprised the following: Ar 30 s; H_2 30 s; Ar 30 s; 30 s O_2; and repeat (Figure 6). The catalyst coated, mixed conducting polymer sample A-4 cycles between fuel (H_2), argon, and oxidizer (O_2) to induce forward bending, and reverse bending as shown in Movie S1, indicating change of oxidation state of the polymers due to the charge injection that caused conformational change along the polymer chain resulting in a stress which in turn bends the membranes. Conducting polymers can be doped and undoped, thus the conductivity and structural conformational change can be utilized for actuation purposes. The average angular speed was recorded by assessing bending angle and time. However, only sample A-4 showed a maximum angle of 90º in 45 seconds with repeatable cycling. It is possible that the layers and formation of PAA agglomerate physically to prevent charge injection into the PANI, thus, preventing conformational change in case of other samples.

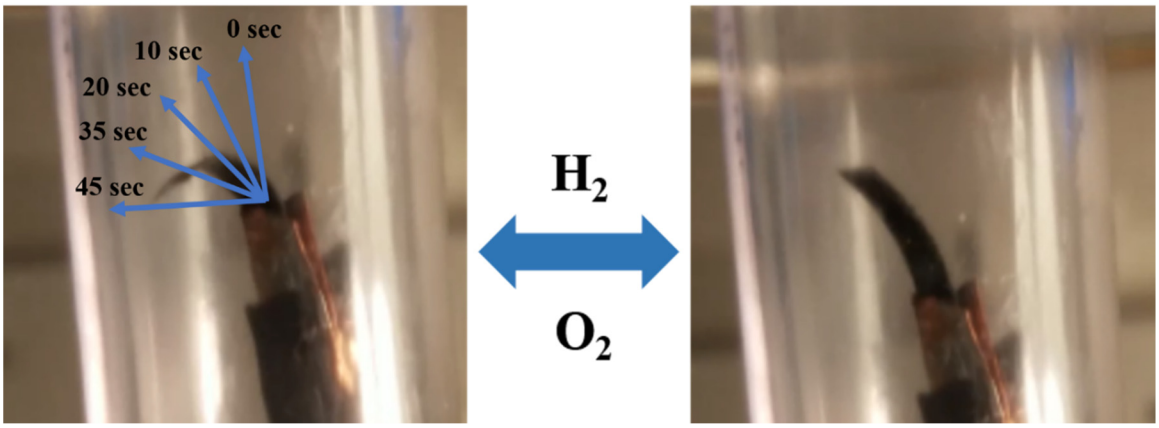

Figure 6 Fuel bending actuation for $PANI_3PAA_1SPEEK_3$ (A-4) under exposure of H_2 (left) and then O_2 (right)

3.3 Moisture absorption

The PANI-PAA-SPEEK composites exhibited a significant moisture absorption capability due to the presence of hydrophilic functional groups including hydroxyl groups (-OH) and amide groups (-NH-) of the PAA and PANI, respectively, by formation of hydrogen bonds with water molecules as shown in Figure 7.[39] The amount of moisture present on human hands at ambient humidity is sufficient to roll up the films swiftly. This material recovers its original state when removed from the hand. This process could be repeated many times which is an indication of flexibility and reversibility (Movie S2).

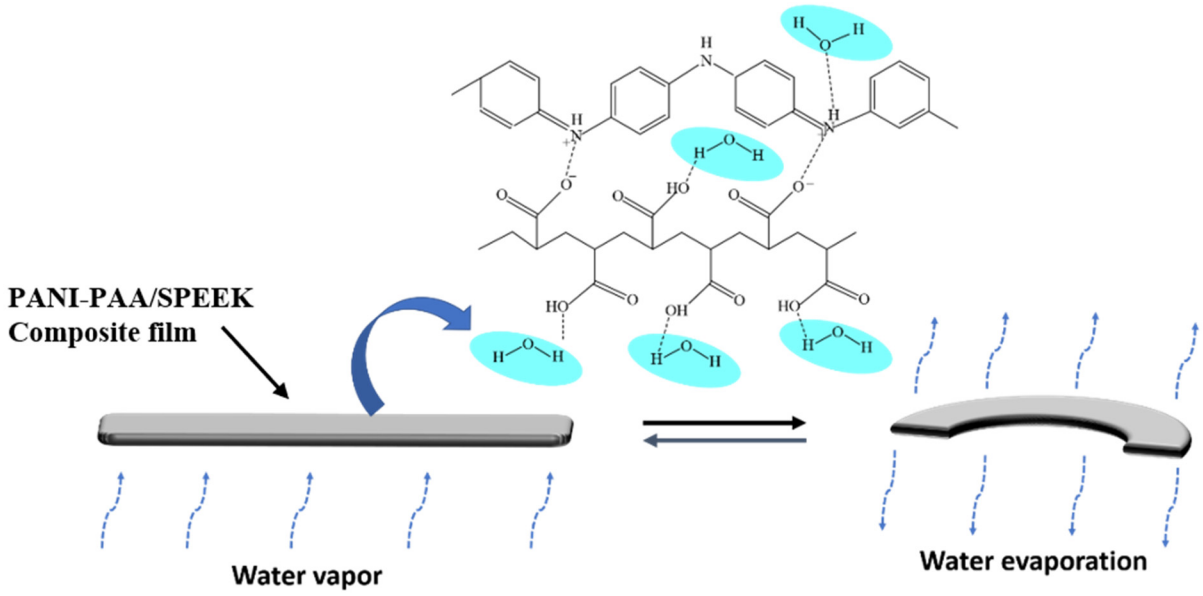

Figure 7 Schematic illustrations of PANI-PAA/SPEEK composite moisture absorption and desorption

Changes in morphology based on moisture absorption can be utilized to provide tensile actuation and work capacity.[40] Sections of the composite films measuring 25 μm in thickness were cut into rectangles (2 cm x 4 cm) and used to measure mechanical actuation due to moisture absorption/desorption. The samples were tested without twisting or forming a helical structure because that is inconvenient in application due to the potential for the formation of side snarls or loose snarls that have detrimental effects on actuation. The mechanical actuation property was evaluated under applied tension of 100 mN by hanging a load at the end of the sheet.

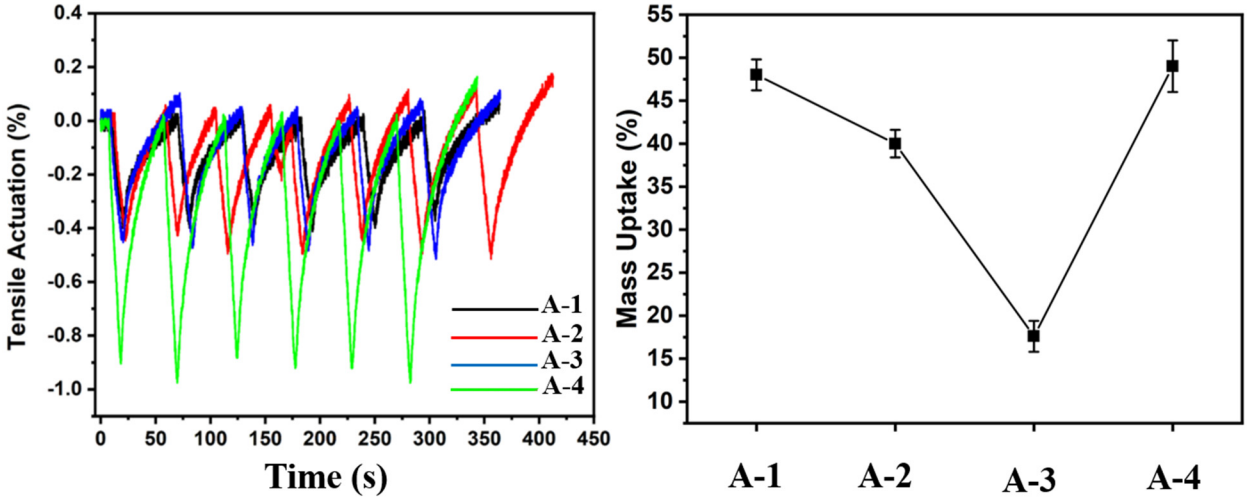

(A) (B)

Figure 8 Tensile test (A), Mass uptake (B); for $PANI_1PAA_1SPEEK_3$ (black, A-1), $PANI_2PAA_1SPEEK_3$ (red, A-2), $PANI_1PAA_2SPEEK_3$ (blue, A-3), and $PANI_3PAA_1SPEEK_3$ (green, A-4)

The films exhibited a rapid axial expansion when exposed to wet air, indicating water absorption. As shown in Figure 8, sample A-4 expanded 3mm in 15 seconds giving a stroke of 1%, higher than all other samples which had strokes in the range of 0.4-0.5 %. The samples return to their original length within 1 minute following exposure to dry nitrogen which caused water molecules to evaporate. The maximal contractile strain remained the same for 8 cycles. The existence of porosity in A-4 D may have enhanced the rate of water molecule exchange between the composite and the environment. Mass uptake is a good indication of proton transfer; however, high swelling means slower reversible contraction. The mass uptake of the composites increases with increasing PAA content, as expected, owing to its capability to form hydrogen bonds. However, the swelling ratio in the case of sample A-3 showed the lowest at 16% followed by 39% for A-2, 47% for A-1, and 50% for A-4. Highest mass uptake of 50% for sample A-4 is consistent with moisture absorption stroke data. This result shows that higher concentration of PAA may result in a higher degree of crosslinking, shortening the molecular distance and creating a stiff structure, which in turn affected the mass uptake and thus results in less actuation performance.

4 Conclusion

A series of PANI-PAA-SPEEK composites were prepared. The optimum composition of $PANI_3PAA_1SPEEK_3$, with excellent mechanical properties, enhanced conductivity ($1.8x\ 10^{-2}$ S/cm), redox potential bending capability, and moisture-based linear actuation is demonstrated. The role of composition is revealed by the mechanical and electrochemical impedance characterizations. A higher tensile strength of 8.4 MPa was obtained for a composite with a higher concentration of PAA, however, the mass uptake, conductivity, and actuation capability were lower for that composition, indicating that $PANI_3PAA_1SPEEK_3$ is more optimal for this application space.

Conflict of Interest

The authors declare no competing financial interest.

Acknowledgements: This work was supported by DEVCOM Army Research Laboratory and was accomplished under Cooperative Agreement Number W911NF-16-2-0008, General Technical Services, contract No. W911QX-20-F-0023, and Fibertek, Inc, contract No. W15P19D0038.

References

1 Byun J, Lee YM, Cho CS. Swelling of thermosensitive interpenetrating polymer networks composed of poly (vinyl alcohol) and poly (acrylic acid). *J Appl Polym Sci.* 1996;61(4):697-702E.

2 Dragan ES. Advances in interpenetrating polymer network hydrogels and their applications. *Pure Appl Chem.* 2014;86(11):1707-21.

3 Bajpai AK, Shukla SK, Bhanu S, Kankane S. Responsive polymers in controlled drug delivery. *Prog Polym Sci.* 2008;33(11):1088-118.

4 Attia NF, Geckeler KE. Polyaniline as a material for hydrogen storage applications. *Macromol Rapid Commun*. 2013;34(13):1043-55.

5 Liu Z, Zhou J, Xue H, Shen L, Zang H, Chen W. Polyaniline/TiO2 solar cells. *Synth Met.* 2006;156(9-10):721-3.

6 Paul EW, Ricco AJ, Wrighton MS. Resistance of polyaniline films as a function of electrochemical potential and the fabrication of polyaniline-based microelectronic devices. *Am J Phys Chem*. 1985;89(8):1441-7.

7 Jeon J-W, Kwon SR, Li F, Lutkenhaus JL. Spray-on polyaniline/poly (acrylic acid) electrodes with enhanced electrochemical stability. *ACS Appl Mater Interfaces*. 2015;7(43):24150-8. J. M.

8 Sansiñena JM, Gao J, Wang HL. High-Performance, Monolithic Polyaniline Electrochemical Actuators. *Adv Funct Mater*. 2003;13(9):703-9.

9 Zhang D, Wang Y. Synthesis and applications of one-dimensional nano-structured polyaniline: an overview. *Mater Sci Eng B*. 2006;134(1):9-19.

10 Guimard NK, Gomez N, Schmidt CE. Conducting polymers in biomedical engineering. *Prog Polym Sci*. 2007;32(8-9):876-921.

11 Zhao Z, Hwang Y, Yang Y, Fan T, Song J, Suresh S, et al. Actuation and locomotion driven by moisture in paper made with natural pollen. Proc. Natl. Acad. Sci. U. S. A. 2020;117(16):8711-8.

12 Ma M, Guo L, Anderson DG, Langer R. Bio-inspired polymer composite actuator and generator driven by water gradients. *Sci*. 2013;339(6116):186-9.

13 Li HQ, Liu XJ, Wang H, Yang H, Wang Z, He J. Proton exchange membranes with cross-linked interpenetrating network of sulfonated polyvinyl alcohol and poly (2-acrylamido-2-methyl-1-propanesulfonic acid): Excellent relative selectivity. *J Member Sci*. 2020; 595:117511.

14 Wang Z, Zhou H, Lai J, Yan B, Liu H, Jin X, et al. Extremely stretchable and electrically conductive hydrogels with dually synergistic networks for wearable strain sensors. *J Mater Chem*. 2018;6(34):9200-7.

15 Baicea C, Luntraru V, Vaireanu D, Vasile E, Trusca R. Composite membranes with poly (ether ether ketone) as support and polyaniline like structure, with potential applications in fuel cells. *Open Chem J*. 2013;11(3):438-45.

16 McKeon-Fischer K, Flagg D, Freeman J. Poly (acrylic acid)/poly (vinyl alcohol) compositions coaxially electrospun with poly (ε-caprolactone) and multi-walled carbon nanotubes to create nanoactuating scaffolds. *Polymer*. 2011;52(21):4736-43.

17 H. B. Schreyer, M. Shahinpoor and K. J. Kim, in *Smart Structures and Materials 1999: Electroactive Polymer Actuators and Devices*, International Society for Optics and Photonics, 1999, pp. 192-198.

18 McKeon-Fischer K, Flagg D, Freeman J. Poly (acrylic acid)/poly (vinyl alcohol) compositions coaxially electrospun with poly (ε-caprolactone) and multi-walled carbon nanotubes to create nanoactuating scaffolds. *Polymer*. 2011;52(21):4736-43.

19 Nemat-Nasser S. Micromechanics of actuation of ionic polymer-metal composites. *J Appl Phys*. 2002;92(5):2899-915.

20 Swift T, Swanson L, Geoghegan M, Rimmer S. The pH-responsive behavior of poly (acrylic acid) in aqueous solution is dependent on molar mass. *Soft matter*. 2016;12(9):2542-9.

21 Lu X, Zhang Z, Li H, Sun X, Peng H. Conjugated polymer composite artificial muscle with solvent-induced anisotropic mechanical actuation. *J Mater Chem*. 2014;2(41):17272-80.

22 Lu W, Qu L, Henry K, Dai L. High performance electrochemical capacitors from aligned carbon nanotube electrodes and ionic liquid electrolytes. *J Power Sources*. 2009;189(2):1270-7.

23 Ho C-H, Liu C-D, Hsieh C-H, Hsieh K-H, Lee S-N. High dielectric constant polyaniline/poly (acrylic acid) composites prepared by in situ polymerization. *Synth Met*. 2008;158(15):630-7.

24 Zhong W, Yang Y, Yang W. Oxidative graft polymerization of aniline on the surface of poly (propylene)-graft-polyacrylic acid films. *Thin solid films*. 2005;479(1-2):24-30.

25 Hu H, Cadenas JL, Saniger JM, Nair P. Electrically conducting polyaniline–poly (acrylic acid) blends. *Polym Int*. 1998;45(3):262-70.

26 (a) Gupta B, Prakash R. Synthesis of processible doped polyaniline-polyacrylic acid composites. *J Appl Polym Sci*. 2009;114(2):874-82. (b) Tong J, Han C, Hao X, Qin X, Li B. Conductive polyacrylic acid-polyaniline as a multifunctional binder for stable organic quinone electrodes of lithium-ion batteries. *ACS Appl Mater Interfaces*. 2020;12(35):39630-8.

27 Wang T, Zhang Y, Liu Q, Cheng W, Wang X, Pan L, et al. A self-healable, highly stretchable, and solution processable conductive polymer composite for ultrasensitive strain and pressure sensing. *Adv Funct Mater*. 2018;28(7):1705551.

28 Syed JA, Tang S, Lu H, Meng X. Water-soluble polyaniline–polyacrylic acid composites as efficient corrosion inhibitors for 316SS. *Ind Eng Chem Res*. 2015;54(11):2950-9.

29 Mirmohseni A, Wallace G. Preparation and characterization of processable electroactive polyaniline–polyvinyl alcohol composite. *Polymer*. 2003;44(12):3523-8.

30 Zhong W, Yang Y, Yang W. Oxidative graft polymerization of aniline on the surface of poly (propylene)-graft-polyacrylic acid films. *Thin Solid Films*. 2005;479(1-2):24-30.

31 Mostafaei A, Zolriasatein A. Synthesis and characterization of conducting polyaniline nanocomposites containing ZnO nanorods. *Prog Nat Sci*. 2012;22(4):273-80.

32 Wang Y, Wang X, Tang S, Vongehr S, Syed JA, Meng X. Highly processible and electrochemically active graphene-doped polyacrylic acid/polyaniline allowing the preparation of defect-free thin films for solid-state supercapacitors. *RSC Adv*. 2015;5(77):62670-7.

33 Bagheri N, Lakouraj MM, Nabavi SR, Tashakkorian H, Mohseni M. Synthesis of bioactive polyaniline-b-polyacrylic acid copolymer nanofibrils as an effective antibacterial and anticancer agent in cancer therapy, especially for HT29 treatment. *RSC Adv*. 2020;10(42):25290-304.

34 Gil-Castell O, Galindo-Alfaro D, Sánchez-Ballester S, Teruel-Juanes R, Badia JD, Ribes-Greus A. Crosslinked sulfonated poly (vinyl alcohol)/graphene oxide electrospun nanofibers as polyelectrolytes. *Nanomaterials*. 2019;9(3):397.

35 Baicea C, Luntraru V, Vaireanu D, Vasile E, Trusca R. Composite membranes with poly (ether ether ketone) as support and polyaniline like structure, with potential applications in fuel cells. *Open Chem*. 2013;11(3):438-45.

36 Ren S, Xu M, Yang Y, Ma S, Hao C. Effects of microstructural functional polyaniline layers on SPEEK/HPW proton exchange membranes. Journal of Applied Polymer Science. 2014;131(21)**.**

37 Vaireanu D-I, Maior I, Grigore A, Savoiu D. The evaluation of ionic conductivity in polymer electrolyte membranes. *Rev Chim*. 2008;59(10):1140-2.

38 Al-Sagur H, Komathi S, Khan M, Gurek A, Hassan A. A novel glucose sensor using lutetium phthalocyanine as redox mediator in reduced graphene oxide conducting polymer multifunctional hydrogel. *Biosens Bioelectron*. 2017; 92:638-45.

39 Yang X, Wang W, Miao M. Moisture-responsive natural fiber coil-structured artificial muscles. *ACS Appl Mater Interfaces*. 2018;10(38):32256-64.

40 Kim SH, Kwon CH, Park K, Mun TJ, Lepró X, Baughman RH, et al. Bio-inspired, moisture-powered hybrid carbon nanotube yarn muscles. *Sci Rep*. 2016;6(1):1-7.